Supporting Information

Du et al. 10.1073/pnas.1417215111

SI Materials and Methods

Generation of *Egr2* Conditional Knockout Mice. To delete the entire *Egr2* coding region by homologous recombination (see schematic in Fig. S1*A*), we amplified the 1,371 bp (herein denoted as 1.4 kb) DNA fragment containing exons 1 and 2, and cloned it 5′ of the neomycin-resistant gene cassette in a gene-targeting vector, pNTK-loxP/FRTII. The 5,356 bp (herein denoted as 5.4 kb) DNA fragment that includes exon 3, containing the entire EGR2 coding region from C57BL/6 BAC DNA, was cloned separately. A LoxP site was inserted in this fragment by site-directed mutagenesis using QuikChange (Stratagene), verified by sequencing, and the mutated 5.4-kb fragment cloned into pNTK-loxP/FRTII containing the 1.4-kb fragment to generate the final pNTK-loxP/FRTII-Egr2CKO targeting vector. This was transfected into 129 embryonic stem (ES) cells, and cells exhibiting homologous recombination were identified by PCR and Southern blotting and injected into C57BL/6 blastocysts. Resulting chimeric mice were mated with C57BL/6 mice, germ-line transmission was confirmed by PCR and Southern blotting, and progeny were crossed sequentially to *FLPe* transgenic and T-cell–specific *CD4*-Cre transgenic mice to delete the neomycin-resistance gene and the *Egr2* coding region, respectively. The primer pairs (*Egr2* CKO-P1: 5′-TGGTCGGCTCTTTTTATTGG-3′, *Egr2* CKO-(Neo)-P2: 5′-ATCGCCTTCTATCGCCTTCT-3′, and *Egr2* CKO-P3: 5′-AACACCCAATAGCAGCAACA-3′) were used to confirm deletion of the neomycin resistance gene. The primer pairs (Cre-531: 5′-CGATGCAACGAGTGATGAGG-3′ and Cre-819: 5′-GCATTGCTGTCACTTGGTCCT-3′) were used to confirm the presence of *CD4*-Cre. $Egr2^{f/f}CD4\text{-}Cre^{-/-}$ mice were used as controls. Mice were backcrossed 8–10 generations to C57BL/6 mice. Animal protocols were approved by the NHLBI Animal Care and Use Committee, following the National Institutes of Health Guidelines "Using Animals in Intramural Research.

Th Polarization. Naïve $CD4^+$ T cells from spleen and lymph nodes were purified from 6-wk-old mice using a $CD4^+CD62^+$ T-cell Isolation Kit II (Miltenyi). Naïve $CD8^+$ T cells were sorted from purified total $CD8^+$ T cells using CD8a (Ly2) beads (Miltenyi). Cells were activated with 2 μg/mL plate-bound anti-CD3 + 1 μg/mL soluble anti-CD28 (PharMingen) with or without 100 IU/mL IL-2. For Th0 conditions, 10 μg/mL anti–IL-4 (11B11) and 10 μg/mL anti–IFN-γ were added; for Th1 and Tc conditions, 10 μg/mL anti–IL-4 (11B11) and 10 ng/mL IL-12 were added; for Th2 conditions, 10 μg/mL anti–IFN-γ and 20 ng/mL IL-4 were added; for Th9 conditions, 10 μg/mL anti–IFN-γ, 40 ng/mL IL-4, and 2 ng/mL TGF-β were added; and for Th17 conditions, 10 ng/mL of IL-6, 2 ng/mL of TGF-β, 10 μg/mL of anti–IL-4, and 10 μg/mL of anti–IFN-γ were added. Mouse IL-12 and IL-4 were from PeproTech, TGF-β and IL-6 were from R&D Systems, human IL-2 was from Roche, and neutralizing antibodies to mouse IFN-γ (XMG1.2) and IL-4 (11B11) were from BD Bioscience. Cells were cultured for 3 d in RPMI medium 1640 containing 10 mM Hepes (pH 7.0), 10% (vol/vol) FBS, 2 mM L-glutamine, antibiotics (complete medium), and 50 μM 2-ME.

***Egr2* Silencing Using siRNAs.** The 2×10^5 WT naïve $CD4^+$ T cells in 200 μL of Accell siRNA delivery medium (Thermo Scientific Dharmacon) were cultured per well in a 96-well tissue culture plate with 2 μg/mL plate-bound anti-CD3 + 1 μg/mL soluble anti-CD28 (PharMingen). Commercially available Accell *Egr2* siRNA (Thermo Scientific Dharmacon) was reconstituted with 1× siRNA buffer (Thermo Scientific Dharmacon) to a stock concentration of 100 μM. From this stock solution 2 μL of *Egr2* siRNA was added to each well and mixed gently. The cells were incubated at 37 °C for 72 h. Accell nontargeting siRNA was used as negative control. After 72 h, supernatants were assayed for IL-2 production by ELISA.

RNA-Seq. RNA-Seq was performed as described (1). Total RNA was extracted from 5×10^6 naïve $CD4^+$ T cells, not stimulated or stimulated with anti-TCR for 1, 4, and 16 h, and double-stranded cDNA was synthesized. After sonication, 250- to 450-bp fragments were isolated with 2% E-Gel (Invitrogen), purified, end-repaired, adaptor added, and PCR-amplified for 17 cycles. PCR products were "barcoded" (indexed) and sequenced on an Illumina HiSEq 2000.

ChIP-Seq. ChIP-Seq assays were performed as described (2) with anti-EGR2 antibody (Covance) or normal rabbit serum. Briefly, sequenced raw reads were mapped to the mouse genome (assembly NCBI37/mm9) with Bowtie 0.12.7, and uniquely mapped reads were retained for further analysis. Nonredundant reads were then mapped into nonoverlapping 200-bp windows, and the location of reads on positive (negative) strand was shifted up to 75 bp upstream or downstream from its 5′ start to reflect the approximate center of the DNA fragments associated with the reads. The reads in each 200-bp window were counted and visualized using the IGV (Integrative Genomics Viewer) browser. MACS (model-based analysis for ChIP-Seq) (3) was used to identify binding sites (peaks) and evaluate their significance. Peak calling parameters were set as follows: mfold = 25, $P = 1 \times 10^{-5}$, λ set = [1000, 5000, 10,000] and *g* size = 1.87×10^9, where "mfold" is the high-confidence "fold enrichment" used for assignment of candidate peaks in the treatment library relative to those of the control library; the *P* value is a user-defined threshold (candidate peaks with *P* values below this threshold are considered meaningful binding sites); "λ set" is a dynamic parameter used to capture local bias and calculate the *P* value; and "*g* size" is the mappable genome size.

Real-Time PCR. qRT-PCR was used to measure gene-specific mRNA expression. Primers and probes were from ABI, and results are relative to *Rpl7*.

Virus Infection. Virus stocks were grown in the allantoic cavity of 10-d embryonated chicken eggs and stored in aliquots at −80 °C. Viral titers in the lungs of infected mice were determined using MDCK cells, and the dose to infect 50% of tissue culture cells ($TCID_{50}$) was calculated using the Reed-Muench formula. Age and sex-matched mice were inoculated intranasally (i.n.) with 10^3 EID_{50} of A/PR/8/34 (H1N1) influenza virus (PR8). For recall responses, mice were inoculated intraperitoneally (i.p.) with 10^7 EID_{50} of the heterologous A/Philippines/2/82 (H3N2) (X-79) influenza virus and 6 wk later challenged i.n. with 5×10^3 EID_{50} of PR8. All studies with live influenza viruses followed standard operating procedures in an approved biosafety level-2 facility.

Measurement of Antiviral $CD4^+$ and $CD8^+$ T Cell Responses. Antiviral $CD4^+$ and $CD8^+$ T-cell responses were analyzed by staining with Brilliant Violet 421-labeled I-A(b)$NP_{311–325}$ tetramer and phycoerythrin (PE)-labeled $D^bNP_{366–374}$ pentamer, respectively. To measure antigen-specific cytokine expression, MLN and lung lymphocytes were stimulated in the presence of 1 μM $NP_{311–325}$ or $NP_{366–374}$ peptide for 4 h, and 1 μL/mL Golgi Plug (BD Biosciences) for the last 3 h.

Flow Cytometry. Cell were stained in PBS containing 0.5% BSA and 0.1% azide using antibodies (BD Biosciences or eBioscience). For intracellular staining of cytokines, cells were permeabilized with the Cytofix/Cytoperm reagent (BD Biosciences), stained with antibodies to intracellular cytokines, and data acquired on a FACSCalibur or FACSCanto II flow cytometer (Becton Dickinson) and analyzed using FlowJo software (Tree Star).

1. Lin JX, et al. (2012) Critical role of STAT5 transcription factor tetramerization for cytokine responses and normal immune function. *Immunity* 36(4):586–599.
2. Liao W, Lin JX, Wang L, Li P, Leonard WJ (2011) Modulation of cytokine receptors by IL-2 broadly regulates differentiation into helper T cell lineages. *Nat Immunol* 12(6):551–559.
3. Zhang Y, et al. (2008) Model-based analysis of ChIP-Seq (MACS). *Genome Biol* 9(9): R137.

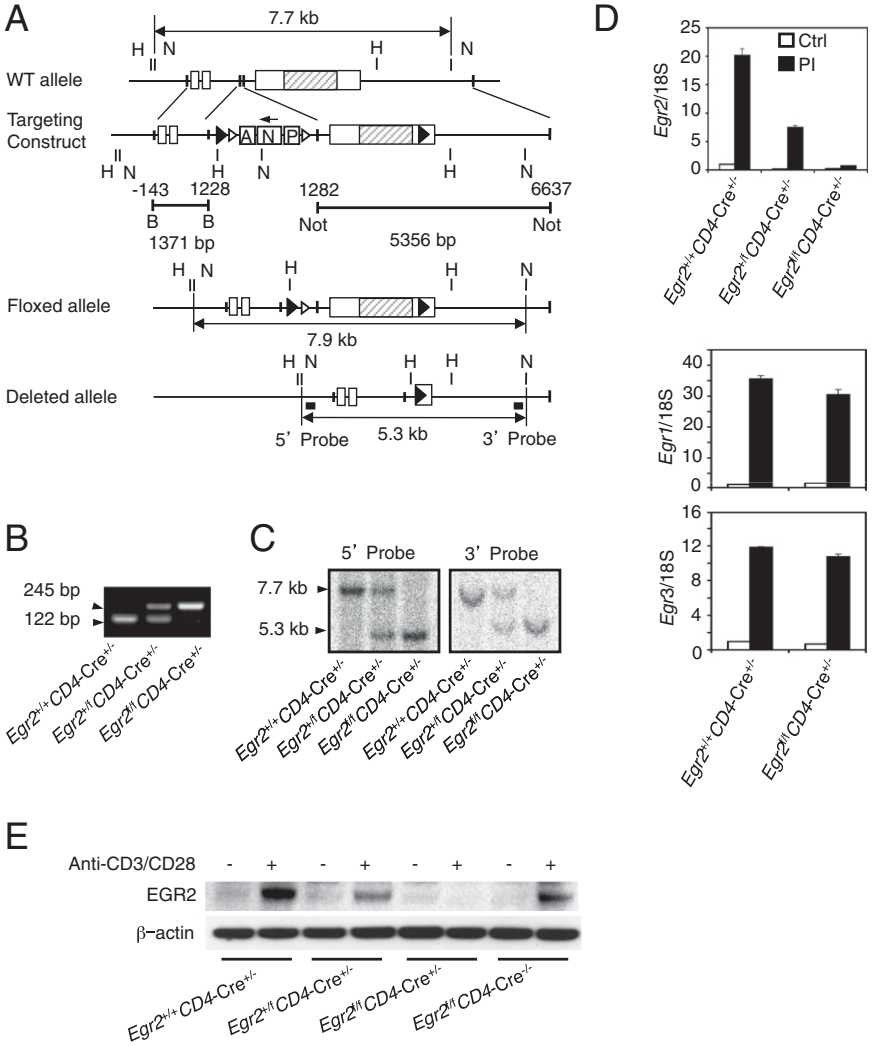

Fig. S1. Generation of *Egr2* CKO mice. (*A*) Targeting strategy. *Egr2* has three exons, with the entire coding region in exon 3 (University of California Santa Cruz Genome Bioinformatics; http://genome.ucsc.edu). Open triangles, FrtII sites; closed triangles, LoxP sites; B, BglII; H, Hind III; N, NcoI; P, phosphoglycerate kinase promoter; N, neomycin transferase; A, bovine growth hormone polyadenylation site. Deleted allele indicates how part of exon 3, including the entire coding region, was deleted by Cre recombinase. The 5′ and 3′ probes are indicated on the bottom schematic. (*B* and *C*) Analysis of Cre-mediated deletion of most of *Egr2* exon 3 in genomic DNA by PCR (*B*) and Southern blotting (*C*) for $Egr2^{+/+}$, $Egr2^{+/f}$, and $Egr2^{f/f}$ alleles. After NcoI digestion, the $Egr2^{+/+}$*CD4*-$Cre^{+/-}$ allele yielded a 7.7-kb DNA fragment; the $Egr2^{f/f}$*CD4*-$Cre^{+/-}$ allele (*Egr2* CKO) lacks exon 3 and yielded a 5.3-kb DNA fragment (*C*). (*D*) Decreased *Egr2* (*Upper*) but not *Egr1* or *Egr3* (*Lower Two* panels) mRNAs in *Egr2* CKO T cells stimulated with PMA + ionomycin for 30 min, as assessed by RT-PCR. (*E*) Western blotting of EGR2 expression in control and *Egr2* CKO cells. Data are representative of one of three independent experiments.

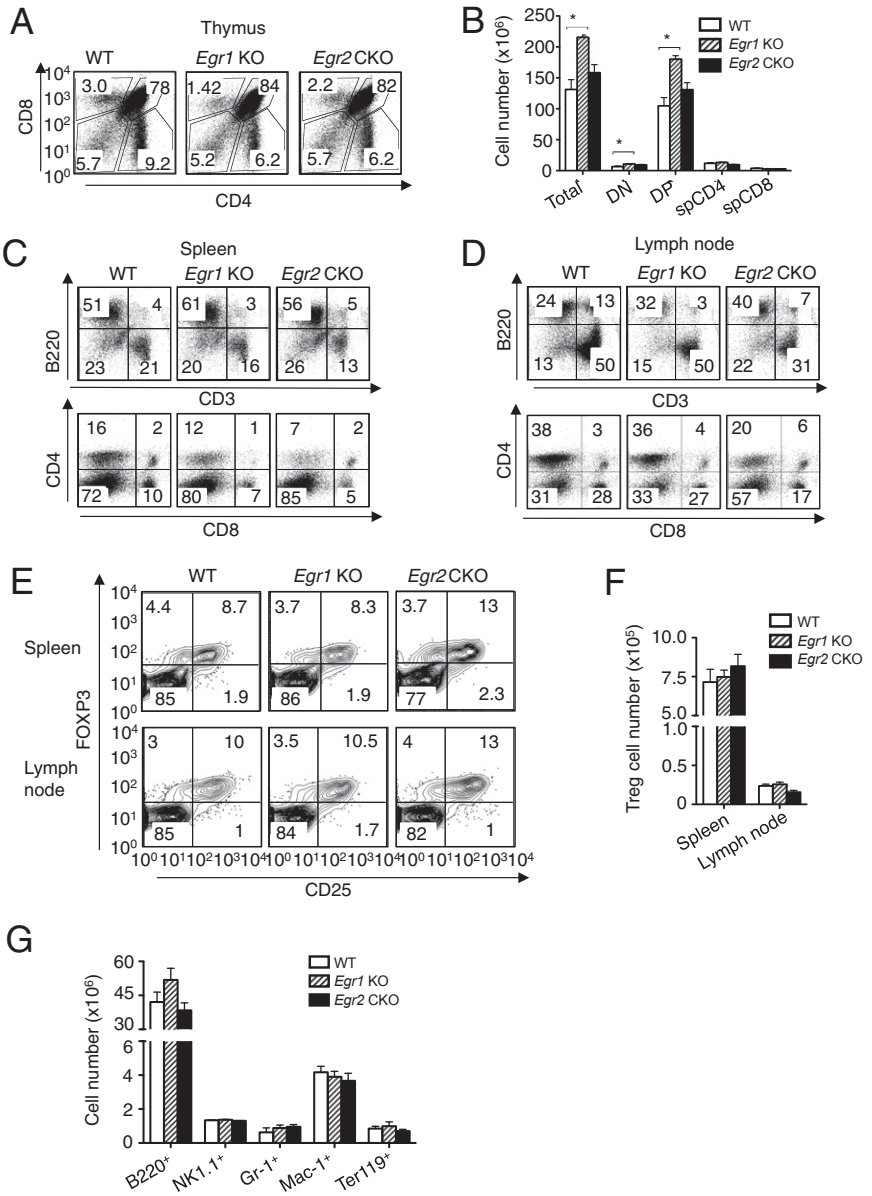

Fig. S2. Similar thymic development in WT and *Egr2* CKO mice. (*A*–*G*) Thymocytes, splenocytes, and lymph node cells were stained as indicated and analyzed by flow cytometry. Representative profiles and cell numbers from 12 mice per group in thymus (*A* and *B*), spleen (*C* and *E*, *Upper*, and *F*), and lymph nodes (*D* and *E*, *Lower* and *F*). (*G*) Numbers of B220$^+$, NK1.1$^+$, Gr-1$^+$, Mac-1$^+$, and Ter119$^+$ cells. Data are from one representative of three experiments with 3 mice per group in each (*A* and *C*–*E*) and three independent experiments (mean ± SD) (*B*, *F*, and *G*).

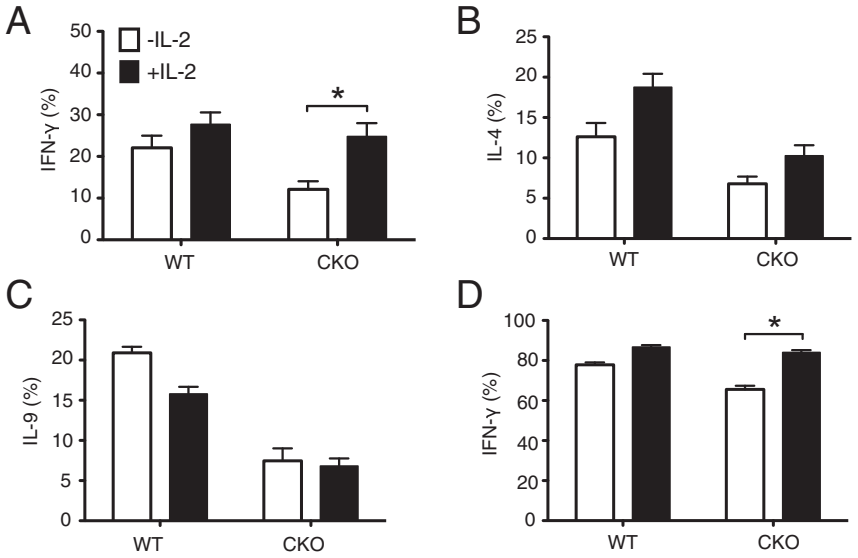

Fig. S3. Exogenous IL-2 can rescue Th1 differentiation in vitro in *Egr2* CKO mice. Naïve $CD4^+$ or $CD8^+$ T cells were differentiated under Th1, Th2, Th9, and Th17 conditions with or without exogenous IL-2 (100 IU/mL), and indicated cytokines were detected by intracellular staining and flow cytometry. Frequency of IFN-γ^+ (*A*), IL-4^+ (*B*), and IL-9^+ (*C*) from naïve $CD4^+$ T cells and IFN-γ^+ (*D*) from naïve $CD8^+$ T cells. Data are representative of three experiments with five mice per group in each (mean ± SD) in *A*–*D*.

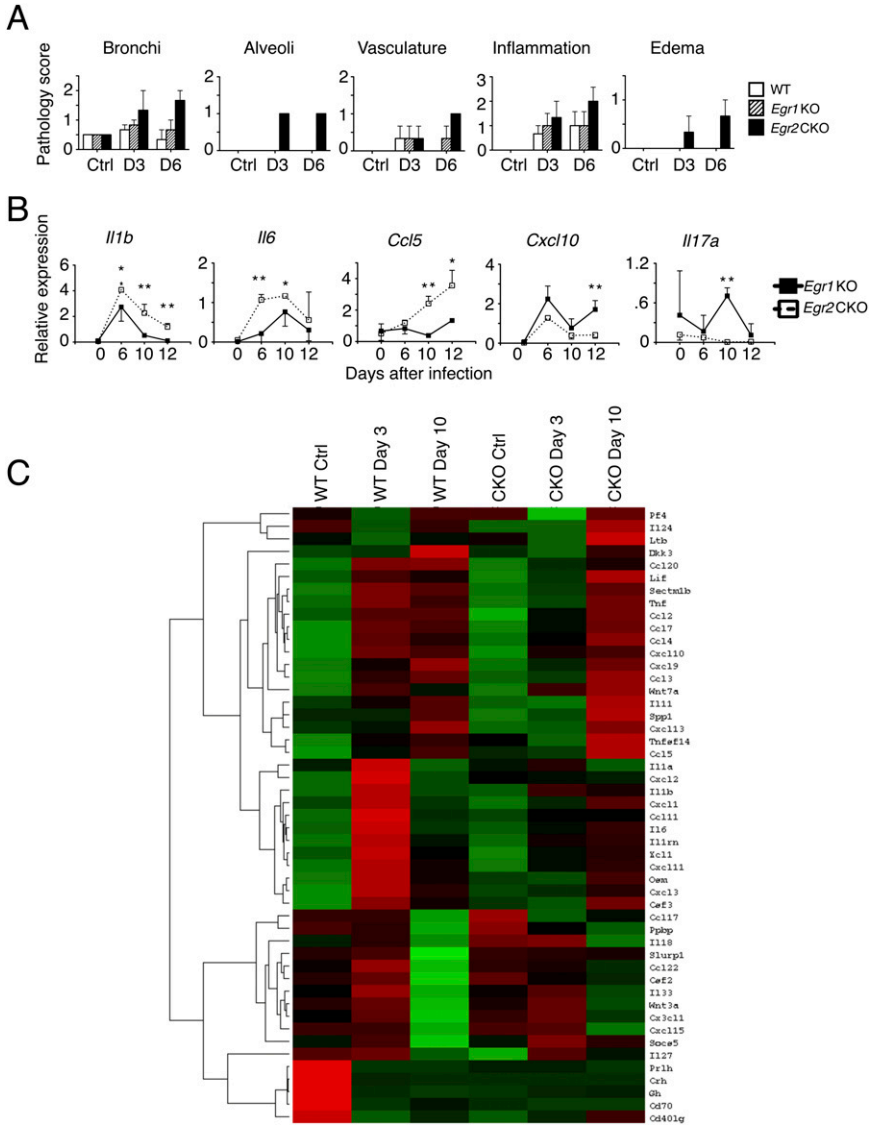

Fig. S4. Greater pathology and altered cytokine/chemokine expression in the lung of *Egr2* CKO mice after influenza infection. (*A*) Pathology scores for bronchi, alveoli, vasculature, inflammation, and level of edema. (*B*) Altered cytokine/chemokine expression in the lungs after primary influenza infection of *Egr2* CKO mice. Lung mRNA was analyzed by RT-PCR for expression of *Il1b*, *Il6*, *Ccl5*, *Cxcl10*, and *Il17a*. (*C*) RNA-Seq was performed in WT and *Egr2* CKO lung cells at days 0, 3, and 10 after primary influenza infection. Heat map of RNA-Seq data for 49 genes with different expression (>1.5-fold difference) in *Egr2* CKO versus WT lung cells. Data are from one of three similar experiments (mean ± SD) in *A* and *B* or are representative of two independent experiments (*C*).

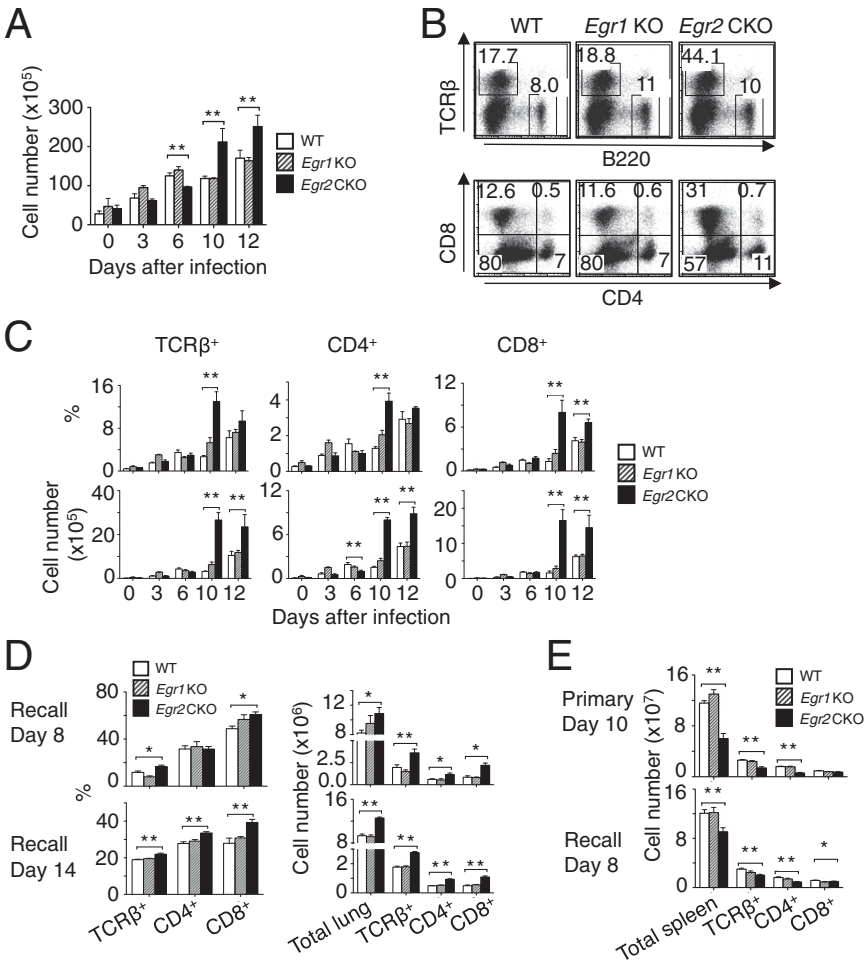

Fig. S5. *Egr2* CKO mice have greater T-cell infiltration of lungs but decreased cells in spleen than wild-type mice after influenza virus infection. Lung cells (*A–D*) and splenocytes (*E*) from WT, *Egr1* KO, and *Egr2* CKO mice were subjected to primary or recall influenza infection models. (*A*) Total lung cells in primary infection model. (*B*) Representative B220/TCRβ, and CD4/CD8 flow cytometric profiles from WT, *Egr1* KO, or *Egr2* CKO T cells in primary infection model. (*C* and *D*) Frequency and total cell numbers in the lungs after primary influenza infection (*C*) or on days 8 and 14 after secondary infection (*D*). (*E*) Total cell numbers in spleens in primary (PR8, d 10) and recall (X-79, PR8, d 8) infection models in WT, *Egr1* KO, and *Egr2* CKO mice. Data are representative of three experiments with five mice per group in each (mean ± SD) in *A* and *C–E* or from one representative of the three experiments in *B*.

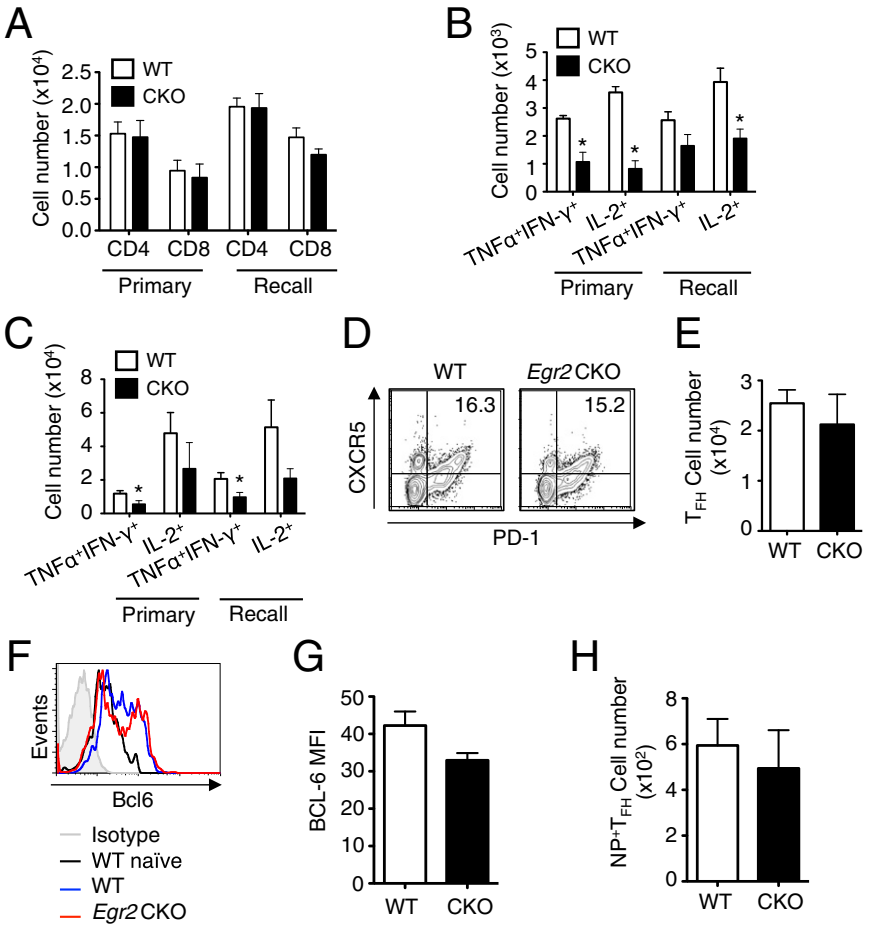

Fig. S6. *Egr2* CKO mice have impaired CD4$^+$ T-cell responses after influenza infection. (*A*) Absolute number of antigen-specific CD4$^+$ and CD8$^+$ T cells in the MLNs in primary and recall models. Absolute number of TNFα$^+$IFN-γ$^+$CD4$^+$ and IL-2$^+$CD4$^+$ T cells in the lungs (*B*) and MLNs (*C*) with NP stimulation for primary and recall models. (*D–H*) T_{FH} cells in MLN were detected after primary infection. (*D*) Representative flow cytometric profiles for CXCR5 and PD-1. (*E*) The number of CXCR5$^+$PD-1$^+$ cells. (*F*) Representative flow cytometric profile for BCL6 expression in CXCR5$^+$PD-1$^+$CD4$^+$ T cells from WT and *Egr2* CKO mice after primary infection. (*G*) MFI of BCL6 and (*H*) the number of antigen-specific T_{FH} cells. Data are representative of three experiments with five mice per group in each (mean ± SD) in *A–C*, *E*, *G*, and *H* or from one representative of the three experiments in *D* and *F*.

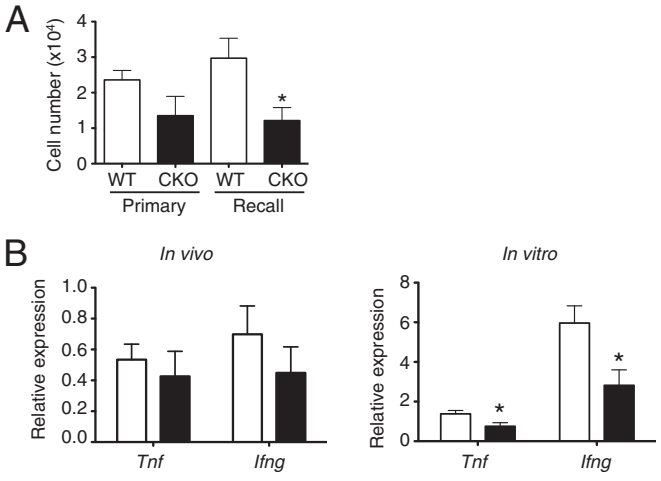

Fig. S7. Impaired CD8$^+$ T-cell response in *Egr2* CKO mice after influenza infection. (*A*) Absolute number of TNFα$^+$IFN-γ$^+$CD8$^+$ T cells in MLNs for primary and recall models. (*B*) Expression of *Tnf* and *Ifng* on T cells from lungs after primary infection (*Left*) and from naïve T cells stimulated with PMA + ionomycin (*Right*). Data are representative of three experiments with five mice per group in each (mean ± SD) in *A* and *B*.

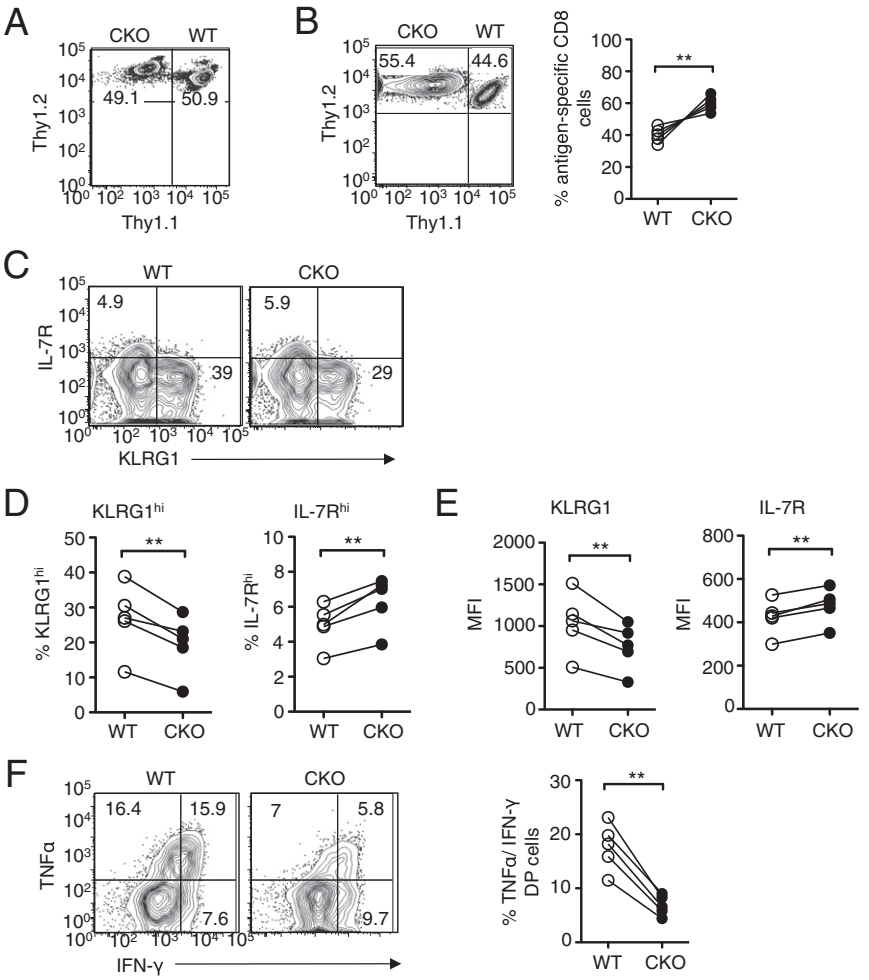

Fig. S8. The *Egr2* CKO P14 cells had similarly defective responses to influenza in Thy1.1 host mice. (*A*) Equal numbers of WT (Thy1.1$^+$Thy1.2$^+$) and *Egr2* CKO (Thy1.1$^-$Thy1.2$^+$) P14 cells were combined and the ratio of the two cell populations was verified by flow cytometry pretransfer into the mice based on differential Thy1.1 and Thy1.2 expression. (*B*) The frequency of P14 cells on day 8 postinfection (because the host is Thy1.2$^-$, the transferred P14 cells are the only Thy1.2$^+$ cells). Representative profile (*Left*) and bar graph (*Right*). (*C–E*) Expression of KLRG1 and IL-7R on WT and CKO P14s. Representative profile (*C*), frequency of KLRG1^{hi} and IL-7R^{hi} P14 cells (*D*) and MFI of KLRG1 and IL-7R (*E*). (*F*) Expression of IFN-γ and TNFα from P14 cells after stimulation with GP33-41 peptide for 5 h, with Golgi-stop added during the last 3 h. Representative profile (*Left*) and frequency of IFN-γ$^+$TNFα$^+$ cells (*Right*). Data are from one of two similar experiments, each of which had five mice per group in *B* and *D–F* (shown is mean ± SD) or from single representative animals in *A–C* and *F*.

Dataset S1. List of all genes differentially expressed in *Egr2* CKO T cells by RNA-Seq analysis

Dataset S1

Dataset S2A. List of 134 genes differentially expressed in *Egr2* CKO T cells that are involved in cell development, growth and differentiation

Dataset S2A

Dataset S2B. Of the 134 genes in Dataset S2*A*, shown are the 36 that directly bind EGR2 based on ChIP-Seq analysis

Dataset S2B